Electronic Supplementary Material (ESI) for New Journal of Chemistry.
This journal is © The Royal Society of Chemistry and the Centre National de la Recherche Scientifique 2018

New Journal of Chemistry

†Electronic Supplementary Information

Boosted Visible Light Photodegradation Activity of Boron Doped rGO/g-C_3N_4 Nanocomposites: The Role of C-O-C Bonds

Shaobo Li [a,b,c], Tao Zhu [a,c], Lichun Dong [a,c] * Mingdong Dong [b] *

[a] School of Chemistry and Chemical Engineering, Chongqing University, Chongqing 400044, China

[b] Interdisciplinary Nanoscience Center (iNANO), Aarhus University, Aarhus-C 8000, Denmark

[c] Key Laboratory of Low-grade Energy Utilization Technologies & Systems of the Ministry of Education, Chongqing University, Chongqing, 40004, China

* Corresponding Authors: Lichun Dong and Mingdong Dong

Tel: +86-23-65106053 (Lichun Dong); +45-8715-6729 (Mingdong Dong)

E-mail address: lcdong72@cqu.edu.cn (Lichun Dong); dong@inano.au.dk (Mingdong Dong)

Mailing address: 221, School of Chemistry and Chemical Engineering, Chongqing University, Chongqing 400044, China (Lichun Dong); Gustav Wieds Vej 14, DK-8000 Aarhus C, Denmark (Mingdong Dong)

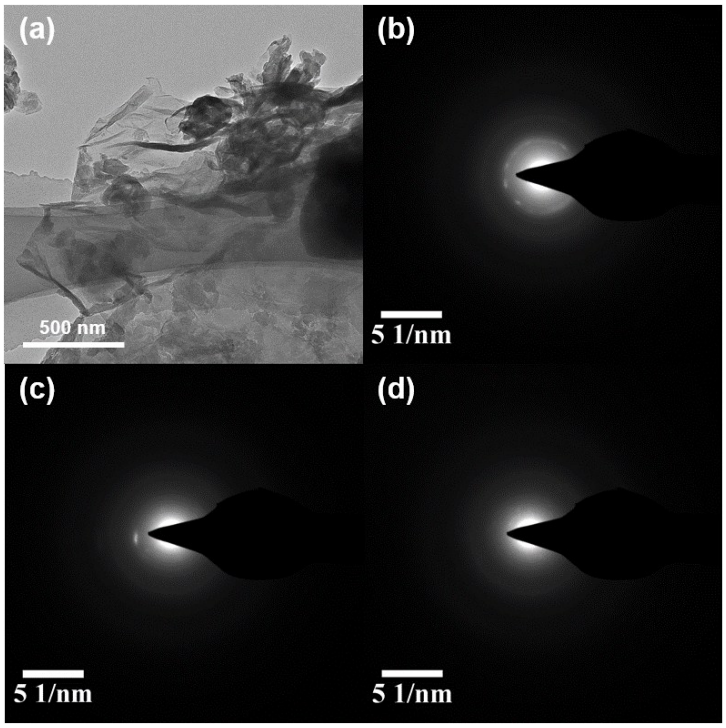

Figure S1. TEM image of 5%rGO/C_3N_4 (a); SAED patterns of g-C_3N_4 (b), 5%rGO/g-C_3N_4 (c) and B-5%rGO/g-C_3N_4 (d).

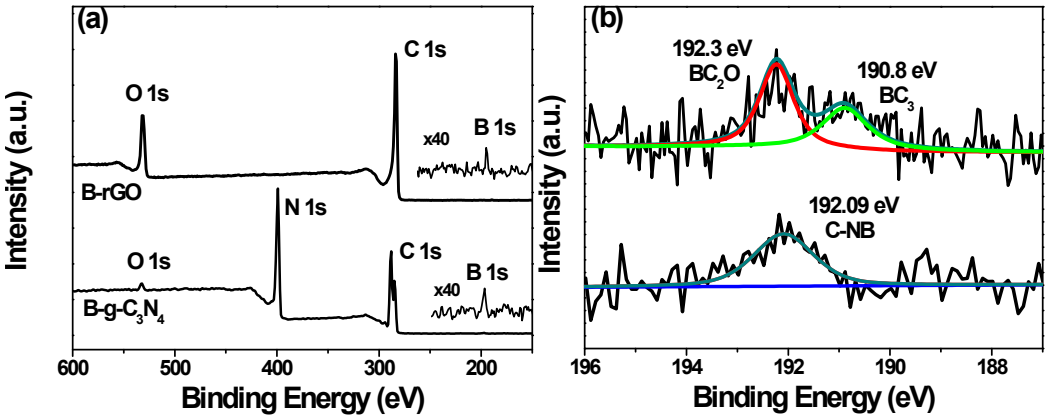

Figure S2. XPS survey (a) and high resolution B1s (b) spectra of B-rGO and B-g-C_3N_4.

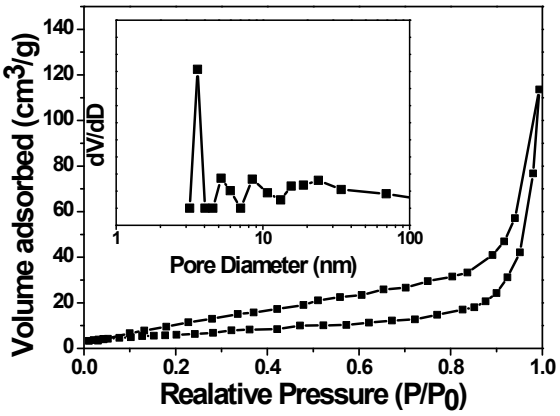

Figure S3. Nitrogen adsorption and desorption isotherms of B-g-C_3N_4 and the inset shows the pore-size distribution.

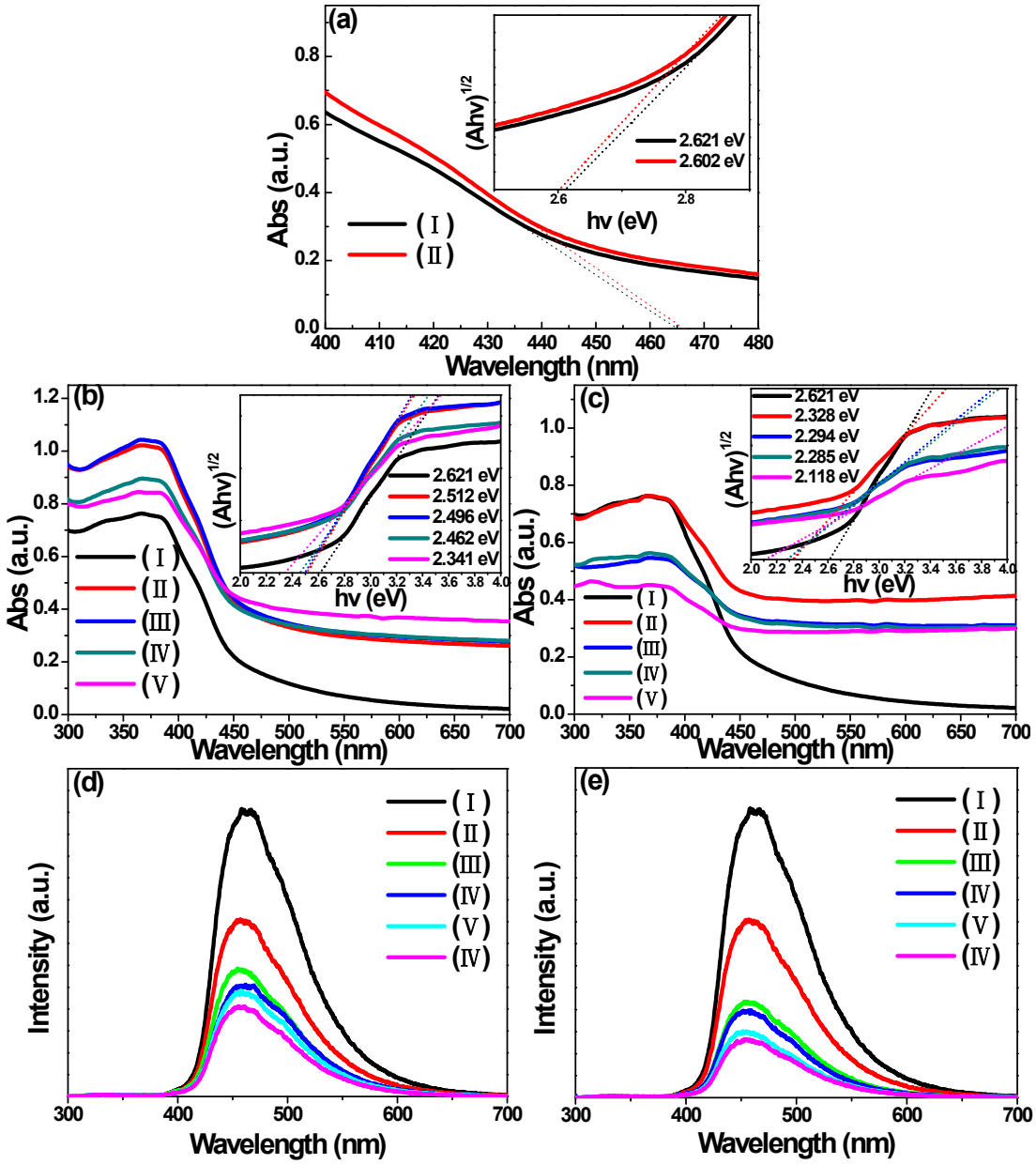

Figure S4. UV-vis diffuse reflectance spectra and the corresponding plots of transformed Kubelka-Munk function versus the light energy (inset) of B-g-C_3N_4 (a) (Ⅰ and Ⅱ refers to g-C_3N_4 without and with B doping), rGO/C_3N_4 (b) and B-rGO/C_3N_4 (c) (Ⅰ to Ⅴ refers to B- rGO/C_3N_4 nanocomposites with different rGO loading: 0%, 1%, 2%, 5% and 10%, respectively); Photoluminescence (PL) spectra of rGO/C_3N_4 (d) and B- rGO/C_3N_4 (e) (Ⅰ to Ⅵ refers to: g-C_3N_4, B-g-C_3N_4 and boron doped g-C_3N_4 nanocomposites with different rGO loading: 0%, 1%, 2%, 5% and 10%, respectively).

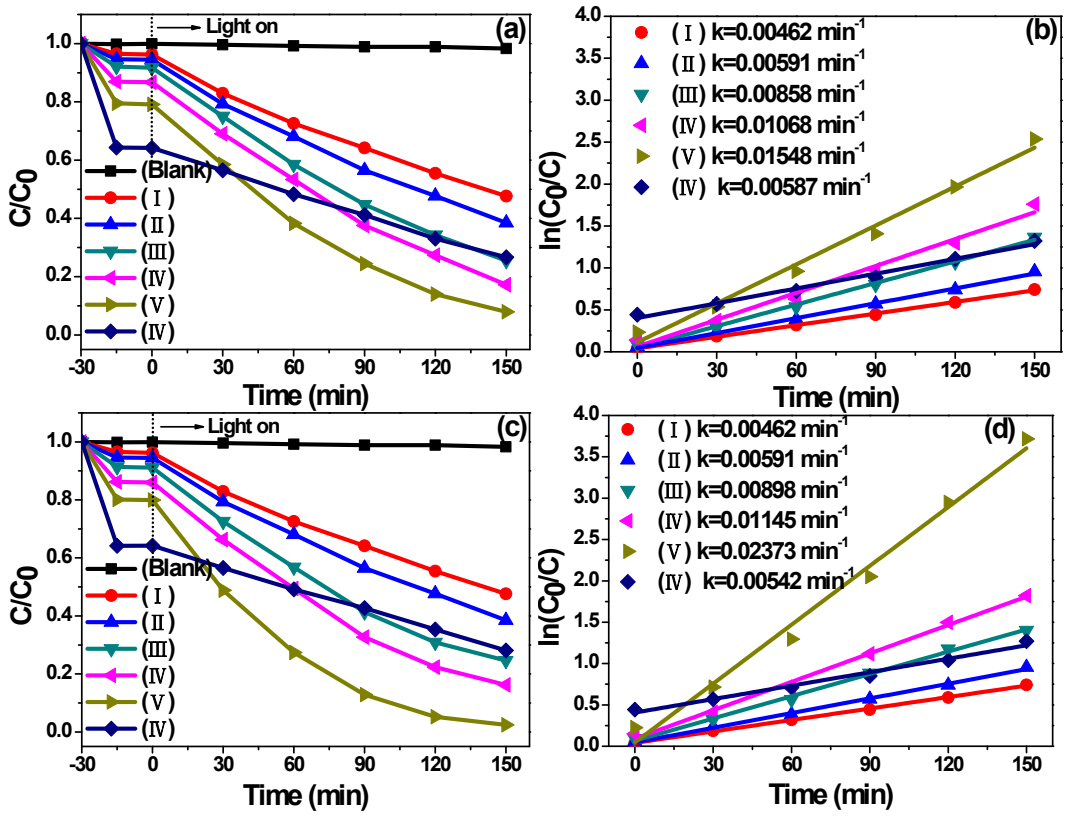

Figure S5. Photocatalytic activity (a) and degradation efficiency (b) for the rGO/C_3N_4 samples ((Ⅰ)-(Ⅵ) represent the pristine g-C_3N_4, B-g-C_3N_4, 1%rGO/C_3N_4, 2%rGO/C_3N_4, 5%rGO/C_3N_4 and 10%rGO/C_3N_4 (d), respectively); Photocatalytic activity (c) and degradation efficiency (d) for the B-rGO/C_3N_4 samples ((Ⅰ)-(Ⅵ) represent the pure g-C_3N_4, B-g-C_3N_4, B-1%rGO/C_3N_4, B-2%rGO/C_3N_4, B-5%rGO/C_3N_4 and B-10%rGO/C_3N_4, respectively).

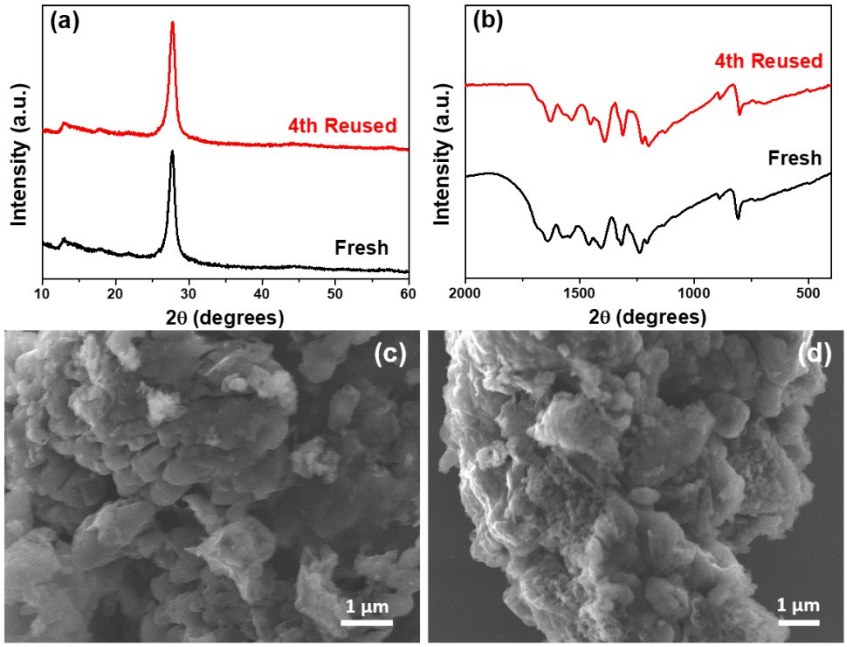

Figure S6. XRD (a), FTIR (b) and SEM images for the fresh (c) and 4th reused (d) B-5%rGO/C_3N_4 samples.

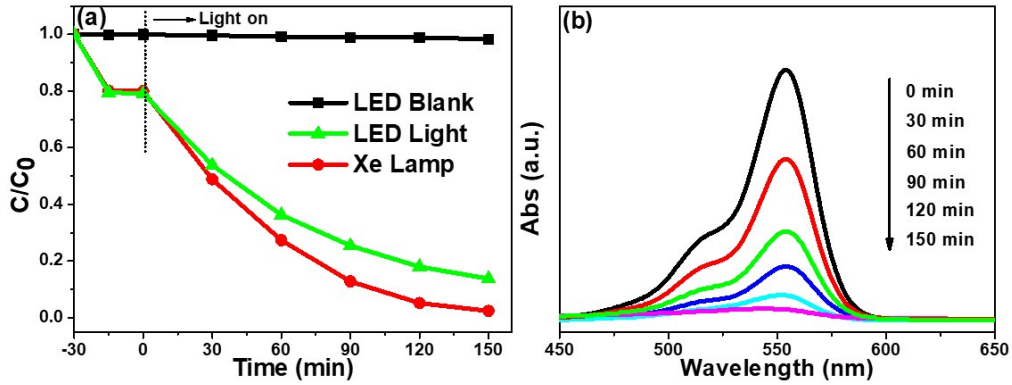

Figure S7. (a) Photocatalytic degradation of RhB under irradiation by different light sources as a function of time over B-5%rGO/g-C_3N_4; (b) The temporal evolution of the spectra during the photodegradation of RhB mediated by B-5%rGO/g-C_3N_4 under 450 nm LED irradiation.

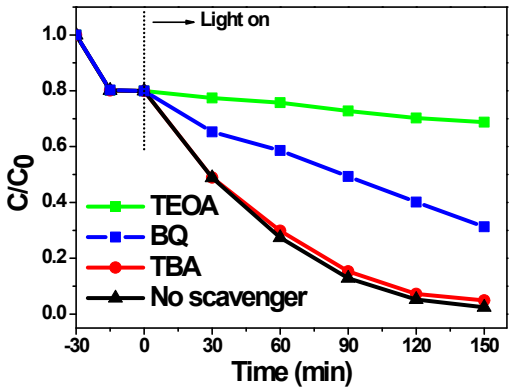

Figure S8. Variation of RhB degradation with time over B-5%rGO/g-C_3N_4 with/without scavengers.